Separation and Purification Technology 380 (2026) 135353

Contents lists available at ScienceDirect

Separation and Purification Technology

journal homepage: www.elsevier.com/locate/seppur

Highly efficient electro-sorption and enrichment of U(VI) from real seawater using modified 3D flexible carbon felt via a flow-through operation

Jiangnan Huang [a,b,1], Shuang Chen [b,1], Yingjie Ruan [b], Hao-Fan Wang [b], Hongjuan Wang [b], Hao Yu [b], Yonghai Cao [b,*]

[a] College of Chemistry and Chemical Engineering, Zhongkai University of Agriculture and Engineering, Guangzhou 510550, China
[b] School of Chemistry and Chemical Engineering, Guangdong Provincial Key Lab of Green Chemical Product Technology, South China University of Technology, Guangzhou 510641, China

ARTICLE INFO

Keywords:
Electro adsorption technology
Flexible carbon felt
Surface modification
U(VI) ions

ABSTRACT

The efficient uptake of U(VI) ions from the real seawater as the nuclear energy source was of paramount importance. Here, the three-dimensional (3D) flexible carbon felts (FCFs) with N dopants and oxygen-containing groups (o-NFCF) were prepared via the solvothermal method. The obtained FCFs were used as the adsorbents for the uptake and enrich of U(VI) by a flow-through electro-sorption operation in the laboratory-designed device. The pristine FCF (pFCF) displayed a 5.0 mg/g capacity under the initial conditions of 10 mg/L U(VI), which was improved with the presence of an electric field (7.2 mg/g, 0.6 V). The o-NFCFs with 2.58 at.% N dopant and 11.09 at.% oxygen functionalities on the surface would lead to the enhanced performance (11.8 mg/g). This was facilitated by the aid of an electric field (18.8 mg/g, 0.6 V) with a Q_{max} of 44.6 mg/g as well. The decreased activity was observed in the simulated seawater (16.4 mg/g) and real seawater (10.6 mg/g), respectively, probably ascribed to the coexistence of organisms and complex ions. The uptake stability of U(VI) from the real seawater was then observed, ascribed to the desorption capability of U(VI) from the surface of o-NFCF. In this process, o-NFCF could be in-situ regenerated simultaneously. By doing so, the enrichment of U(VI) to 5.85 mg/L concentration from a real seawater was obtained. Mechanistic studies and DFT simulations indicated that the electrochemical properties of 3D-NFCF materials dominated the electro adsorption of U(VI).

1. Introduction

The ever-increasing human industrial activities have consumed a vast amount of fossil energy, leading to severe environmental pollution and the significant amount of CO_2 emission [1]. Exploring and developing new types of energy become an inevitable choice for the national development. As the low-carbon energy source, nuclear energy represented by uranium fission is always regarded as an alternative to fossil fuels and the main choice for energy transition [2]. Nevertheless, it is estimated that about 1.5 million tons of terrestrial uranium ores exist, which could only supply the nuclear power plants for less than 100 years [3–5]. Meanwhile, more than 4.5B tons of uranium is believed to be existed in the ocean, which could provide energy for nuclear power plants for at least 10,000 years [4,6,7]. In recent years, the development of novel technologies for extracting uranium from the ocean is urgent issue for countries to seize the initiative in the utilization of nuclear energy. However, the extremely low concentration of uranium (~3.3 μg/L) and other coexisted interfering ions (i.e., Na^+ ions) in real seawater cause significant challenges for the efficient uptake of uranium [7–9]. Therefore, the development of efficient and highly selective technologies for extracting uranium from seawater was of great importance.

In the past decades, various technologies for extracting uranium have been developed, such as adsorption, electroadsorption and electrochemical methods for the extraction of U(VI) [4,5,10–12]. Among them, the electroadsorption technology was a very promising uranium extraction technology due to its low energy consumption, high efficiency and in-situ regeneration ability [13–15]. In this process, the

* Corresponding author.
E-mail address: meyhcao@scut.edu.cn (Y. Cao).
[1] These authors contributed equally.

https://doi.org/10.1016/j.seppur.2025.135353
Received 30 July 2025; Received in revised form 13 September 2025; Accepted 23 September 2025
Available online 25 September 2025
1383-5866/© 2025 Elsevier B.V. All rights are reserved, including those for text and data mining, AI training, and similar technologies.

migration of U(VI) to the surface of adsorbents forming an electric double layer could be accelerated with the aid of an electric field, thus improving the capacitive adsorption [16]. For instance, Wang et al. reported that the electro adsorption capacity of U(VI) could be facilitated over the porous adsorbent with conductive chains, displaying 13.0/16.5 mg/g after 56/90 days [10]. Li et al. used FeOOH/Ni@P foam with a hydrophilic and uranium-affinitive surface as the adsorbent for the extraction of U(VI), exhibiting a capacity of 13.2 mg/g in 7 days with the presence of an electric field [13]. Nevertheless, the conventional electroadsorption technology usually faces the challenge of the limited diffusion ability as well as the adsorption capability. Therefore, the electro adsorption process using Flow-through mode to improve the activity. In this process, the solution was forced to pass through the adsorbent and improved the diffusion of ions inside the adsorbent and the interactions between ions and the adsorbent [17,18]. Meanwhile, with the assistance of an electric field, the interactions between ions and adsorbents would be further strengthened, thereby improving overall performance. For example, Liu et al. developed a highly efficient capacitive deionization system with a Flow-through operation using MoC@CNFAs as the electrodes, exhibiting excellent performance with 37.03 mg/g capacity [19]. Shin and co-workers applied graphitized nanodiamonds-modified electrode as the cathode for the Cr(VI) removal in a flow-through mode, demonstrating high Cr removal capacity (39.51 μmol/g) [20]. Our previous work also demonstrated that the adsorption capacity for the metal ions could be efficiently improved in a flow-through operation [21–23]. Based on this technical foundation, it might be feasible to use the Flow-through mode to adsorb and extract ions from aqueous solution with the aid of an electric field and effectively concentrate them [21,23]. Meanwhile, although the considerable achievements in this filed has been made, two challenges still exist: (i) the influence of impurities in the seawater on the adsorption capability is ignored. Real seawater contains not only competing ions (cations and anions), but also the biofouling challenges i.e., microorganisms, which would significantly influence the electro adsorption capability of U(VI) from real seawater. (ii) The efficient release and enrichment of U(VI) into the specified solution with the in-situ adsorbent regeneration was not well investigated. Although many investigations revealed that their adsorbent would be favorable for the adsorption of U(VI) with the high capacities, how to efficiently desorb the U(VI) from adsorbent surface and enrich it in a specified solution is not fully studied. Simultaneously, the adsorbent could be in-situ regenerated without complex process.

In this study, the flexible carbon felt (FCF) adsorbents were prepared and combined with a laboratory-designed electroadsorption device to achieve the adsorption and enrichment of low-concentration U(VI) in seawater. Our previous study demonstrated that the FCF materials could tightly adhere to the electrode, displaying a high efficiency on the electro adsorption of Pt ions with the in-situ regeneration capability. Here, after optimizing the adsorption conditions such as initial pH, initial concentration and constant potential, the adsorption capacities of U(VI) in pure solution, simulated seawater, and real seawater were explored. The enhanced activities and in-situ regeneration of FCFs material with the presence of an electric field were observed across these systems. By doing so, the enrichment of U(VI) from the real seawater could be achieved. Mechanism study and DFT simulations indicated that the surface physicochemical properties of the carbon adsorbent dominated the electroadsorption. Although the concentration of U(VI) in this work was higher than 3.3 μg/L, this study was not only examine the performance of electroadsorption of U(VI) at low concentration, but also showed activity differences between the pure water, simulated seawater and real water, and investigate the influence of these impurities on the adsorption activity. Meanwhile, the feasibility of our strategy to extract U(VI) from the real seawater with the in-situ regeneration of adsorbent would be revealed as well.

2. Experimental section

2.1. Materials and chemical reagents

The carbon felt (p-FCF, SY-1001) was purchased from Nantong Senyou Carbon Fiber Co., Ltd. Sodium chloride (NaCl, AR), disodium ethylenediaminetetraacetate (Na_2EDTA, AR), azoarsen III ($C_{22}H_{18}As_2N_4O_{14}S_2$, AR), and formamide ($CH_3NO$, AR) were obtained from Aladdin Reagents Co., Ltd. Anhydrous sodium sulfate (Na_2SO_4, AR) and uranyl nitrate hexahydrate ($UO_2(NO_3)_2{\cdot}6H_2O$, AR) were purchased from Shanghai Macklin Biochemical Co., Ltd. Anhydrous ethanol (C_2H_5OH, 99.7 %) and hydrochloric acid (HCl, AR) were obtained from Guangzhou Chemical Reagent Factory. GY-H2 Isochrysis zhangjiangensis (GY-H2IZ) was obtained from the Shanghai Guangyu Biotechnology Co., Ltd. All purchased materials and reagents were used directly without further treatment. The real seawater was obtained from the Pearl River Port in Guangdong Province, China, which was filtered by the membrane with the pore size of 0.2 μm.

2.2. 3D FCFs modifications

Nitrogen-doped flexible carbon felt (NFCF): In general, the p-FCF and formamide were charged in a hydrothermal autoclave and subjected to a temperature of 160 °C for 12 h. The obtained solid carbon was subsequently washed with DI water and dried overnight. Afterward, the solid carbon adsorbent was placed in a tube furnace and heated to 900 °C at a rate of 10 °C/min under a N_2 atmosphere for 2 h.

Nitrogen-doped and oxygenated flexible carbon felt (o-NFCF): In general, the p-FCF, water, and formamide were charged in a hydrothermal autoclave and subjected to a temperature of 160 °C for 12 h. The resulting solid carbon was subsequently washed with deionized water/alcohol and dried overnight. Afterwards, the solid carbon adsorbent was placed in a tube furnace and heated to the 900 °C at a rate of 10 °C/min under a N_2 atmosphere for 2 h. The typical process is illustrated in Fig. 1a. The ratio of Vformamide and Vwater was changed to vary the surface property of o-NFCF-x (x was the ratio of $V_{formamide}/V_{water}$).

2.3. Adsorption performance

The performance and mechanism of efficient adsorption and recovery of U(VI) were explored using an independently designed electrosorption apparatus in the laboratory. The operation process of the apparatus was as follows: A peristaltic pump drew the waste liquid from a beaker and propelled it upward through the flow-through electrosorption unit. The solution was forced to percolate through the carbon material in batch mode before returning to the beaker, thereby achieving cyclic adsorption. The carbon felt was conveniently trimmed to the required dimensions to act as an electrode sheet, which was straightforward and adaptable, ensuring intimate contact with the titanium electrode plate. It was pressed firmly against the counter and reference electrodes of the electrochemical workstation, while a narrow gap separated it from the working electrode positioned below. The volume of the adsorption solution was set at 400 mL. When the peristaltic pump operated at 20 mL/min, the linear velocity of the liquid through the carbon matrix reached 18.1 L/h. After adsorption, a solution sample was taken, which was measured by the UV spectrophotometer using Azotrope III as the chromogenic reagent to determine the concentration of U(VI) ions (Fig. S1).

The biofouling study was carried out as following. 0.12 g o-NFCF was immersed into 4 L real seawater with 10 mg/L U(VI) for 3 days, which contained 800 μL GY-H2IZ. After that, the o-NFCF was put into the device, and the electro adsorption was then carried out.

The specific electrosorption capacity (Q_t, mg/g) was calculated using the following Eq. (1):

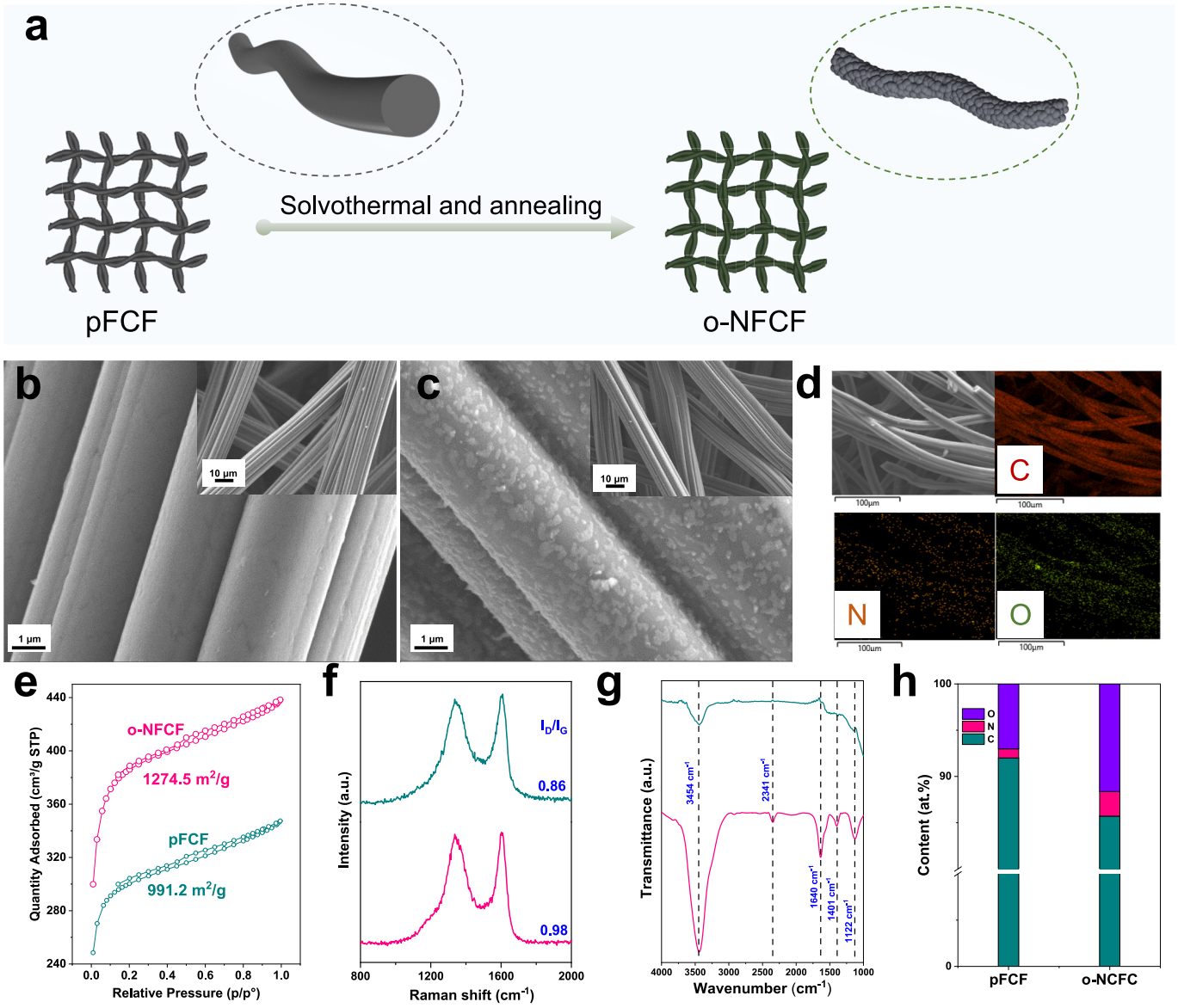

Fig. 1. (a) Schematic illustration of the synthesis of o-NFCF in this study. SEM images of pFCF (b) and o-NFCF (c). (d) SEM-EDS images of the adsorbent. The N_2 adsorption/desorption isotherms (e), Raman spectra (f), FTIR (g), and element content from XPS analysis (h) of pFCF and o-NFCF.

$$Qt = \frac{(C_o - C) \times Vol}{m} \quad (1)$$

where C_o and C are the initial and final concentrations of the target adsorbate (mg/L), *Vol* is the total volume of the pollutant solution (L), and m is the mass of the adsorbent (g).

The adsorption kinetics were fitted using pseudo-first-order and pseudo-second-order models (Eqs. (2)–(3)).

Pseudo-first-order:

$$\log(Q_e - Q_t) = \log Q_e - \frac{k_1}{2.303} t \quad (2)$$

Pseudo-second-order:

$$\frac{t}{Q_t} = \frac{1}{k_2 Q_e^2} + \frac{t}{Q_e} \quad (3)$$

where Q_e (mg/g) and Q_t (mg/g) are the adsorption capacities at equilibrium and at certain time, respectively. t (min) is the adsorption time, and k_1 (min^{-1}) and k_2 (mg/g·min) are the rate constants for the pseudo-first-order and pseudo-second-order equations, respectively.

The adsorption isotherms were fitted using Langmuir and Freundlich isotherms (Eqs. (4)–(5)).

Langmuir isotherm:

$$\frac{C_e}{Q_e} = \frac{1}{K_L Q_{max}} + \frac{C_e}{Q_{max}} \quad (4)$$

Freundlich isotherm:

$$\log Q_e = \log K_F + \frac{1}{n} \log C_e \quad (5)$$

where Q_e (mg/g) and Q_{max} (mg/g) are the equilibrium adsorption capacities and the maximal adsorption capacity, respectively. K_L (L/mg) was the Langmuir constant related to the affinity of binding sites. K_F and n were the Freundlich constants, related to the adsorption capacity of adsorbent and adsorption intensity, respectively.

2.4. Recyclability

The cyclic tests were divided into adsorption and in-situ desorption processes: (1) **Adsorption process:** In this process, U(VI) was used as

the radioactive metal model, and modified 3D-FCF was used as the adsorbent. The experiments were conducted using the self-designed electro adsorption apparatus. At regular intervals, a solution sample was taken to determine concentration of U(VI) by the UV spectrophotometer using Azotrope III as the chromogenic reagents; (2) **Desorption process:** On the same adsorption apparatus, the electrodes were reversed and a voltage of 1.5 V was applied. A 400 mL desorption solution of 0.1 mol/L Na_2SO_4 at 80–90 °C was passed through unidirectionally at a flow rate of 5 mL/min to regenerate the electrodes.

2.5. U ion concentration and extraction process

The adsorption operation was conducted in 1000 mL of real seawater with a U(VI) concentration of 1 mg/L at a voltage of 0.8 V. During desorption, a 100 mL desorption solution of 0.1 mol/L Na_2SO_4 at 80–90 °C was passed through the adsorbed material under a reversed voltage of 1.5 V. The desorption solution was reused in cycles to concentrate the adsorbed U(VI) ions into the same solution. After that, a small amount of solution was taken from the beaker, which was measured by the UV spectrophotometer using Azotrope III as the chromogenic reagent to determine the concentration of U(VI) ions.

2.6. Electrochemical measurements

Cyclic voltammetry (CV) was used to determine the electrical double-layer capacitance. Experiments were conducted at a scan rate of 1 mV/s between −0.5 V and 0.1 V using a 1 cm × 1 cm carbon-felt electrode in 10 mg/L U(VI) solution. The specific capacitance (C) was extracted from the voltammogram according to the Eq. (6):

$$C = \frac{\int_{V_1}^{V_2} IdV}{2mv(V_2 - V_1)} \quad (6)$$

where C is the gravimetric capacitance (F/g), I the response current (A), m the mass of active material (g), v the scan rate (V/s), and ($V_1 \sim V_2$) the potential window (V).

Electrochemical impedance spectroscopy (EIS) complemented the CV measurements by probing the resistance characteristics of the electrode. Spectra were recorded at the open-circuit potential from 10^{-2} to 10^6 Hz, with an AC amplitude of 50 mV, in 0.1 M Na_2SO_4 electrolyte.

2.7. Simulations

The graphene plane and uranium dioxide ion were used to simulate the adsorption behavior on the surface of carbon adsorption. The periodic system for all calculations was applied, in which all calculations were implemented by the Dmol3 package with GGA/PBE correlation exchange function [24,25]. Spin unrestricted setting was checked in calculations. Double numerical plus polarization (DNP) and DFT semi-core pseudopotentials(DSPP) were used to describe the atomic orbital and core electrons, respectively [26]. In this work, the DFT-D method introduced by Grimme was employed to overcome the long-range dispersion [27]. The k-point was set to be 2 × 2 × 1 for sampling the Brillouin zone. And the convergence tolerance of energy, force and displacement were 1.0 × 10^{-6} Ha, 0.02 Ha $Å^{-1}$ and 0.005 Å, respectively. The adsorption energy (ΔE) of adsorbate (A) on substrate was calculated by the following Eq. (7):

$$\Delta E = E_{A-substrate} - E_A - E_{Substrate} \quad (7)$$

where the $E_{A\text{-substrate}}$, E_A and $E_{Substrate}$ were the total energies of the molecule A adsorbed system, the free molecule A and substrate material, respectively. In addition, the more negative the value of ΔE, the more favorable the substrate adsorption to A.

3. Results and discussions

3.1. Materials and characterizations

o-NFCF was prepared through the hydrothermal-annealing processes, which significantly altered the physicochemical properties of the carbon material's surface (Fig. 1a). SEM images demonstrated that the surface of the pFCF was smooth without obvious defects or wrinkles (Fig. 1b). In contrast, the surface of the modified o-NFCF was covered with numerous small particles (∼ 200 nm in size) (Fig. 1c). This indicated that the surface of the carbon adsorbent could be efficiently varied via the solvothermal process. EDS analysis revealed that the well-distributed elements i.e., N and O, on the carbon surface were observed, indicating that the incorporation of N dopants and oxygen-containing groups was achieved, thus alerting the chemistry property of surface (Fig. 1d). Furthermore, the specific surface area (SSA) of the pFCF was approximately 991.2 m^2/g, while that of o-NFCF increased to 1274.5 m^2/g, nearly a 1.3-fold increase (Fig. 1e). Meanwhile, Raman spectra showed that the I_D/I_G ratio of o-NFCF was 0.98, higher than that of pFCF (0.86), suggesting that the surface of o-NFCF contained a large number of defects, which could afford more active adsorption sites (Fig. 1f). FTIR characterization results revealed that the peaks at 3454 cm^{-1}, 1640 cm^{-1}, 1401 cm^{-1}, and 1122 cm^{-1}, corresponding to the stretching vibrations of hydroxyl (O—H) group, carbonyl (C=O) group, carboxyl (C—O) group, and ether/ester (C—O) group, respectively (Fig. 1g) [28]. The pFCF displayed a low content of these oxygen functionalities on the surface, whereas the modified carbon material (o-NFCF) exhibited a significant increase in several functional groups such as hydroxyl and carboxyl groups, which resulted in the hydrophilic surface on carbon [21,22]. XPS analysis further showed that the carbon material was primarily composed of C, N, and O (Fig. 1h). The pFCF surface contained a small amount of N dopants (1.15 at.%) due to the use of polyaniline as a precursor. Meanwhile, 7.31 at. % of O content in pFCF was observed as well. In contrast, the content of O (11.09 at.%) and N (2.58 at.%) on the o-NFCF surface increased significantly during the modification process. Meanwhile, the surface hydrophilicity/hydrophobicity property of the adsorbents were tested via the contact angle measurement, and we found the o-NFCF displayed lower contact angle (0°) than that of pFCF (127.5°) (Fig. S2), demonstrating that the surface modification could efficiently change the surface physical/chemical properties, which were of great significance for enhancing the adsorption performance.

3.2. Electro adsorption performance

The electro adsorption with a Flow-through model was employed to effectively enhance the diffusion of ions inside the adsorbent, thereby promoting their interaction and improving adsorption efficiency [20,21,23,29]. In this experiment, a Flow-through electrosorption apparatus by self-designed and fabricated using FCF materials as adsorbents in our lab was utilized (Fig. 2a). The carbon material was placed in close contact with the working electrode to ensure optimal electrical conductivity, which in turn enhanced adsorption performance. During this process, pFCF and o-NFCF were used as the typical adsorbents for the adsorption of U(VI) (Fig. 2b). The results demonstrated that when pFCF was used as the adsorbent, the presence of an electric field showed a negligible impact on the adsorption capacity, which slightly increased from 5.0 to 7.2 mg/g. In contrast, o-NFCF exhibited higher adsorption capabilities than that of pFCF, regardless of whether an electric field was applied. Notably, when a applied voltage of 0.6 V was used, the adsorption capacity of o-NFCF reached 18.8 mg/g, 1.6 times of that without an electric field (11.82 mg/g) and 2.6 times higher than that of pFCF with an electric field (7.2 mg/g), demonstrating the unique electrosorption activity of o-NFCF for the uptake of U(VI). These findings suggested that the introduction of oxygen-containing groups and N doping on the surface indeed strengthen the interactions between the

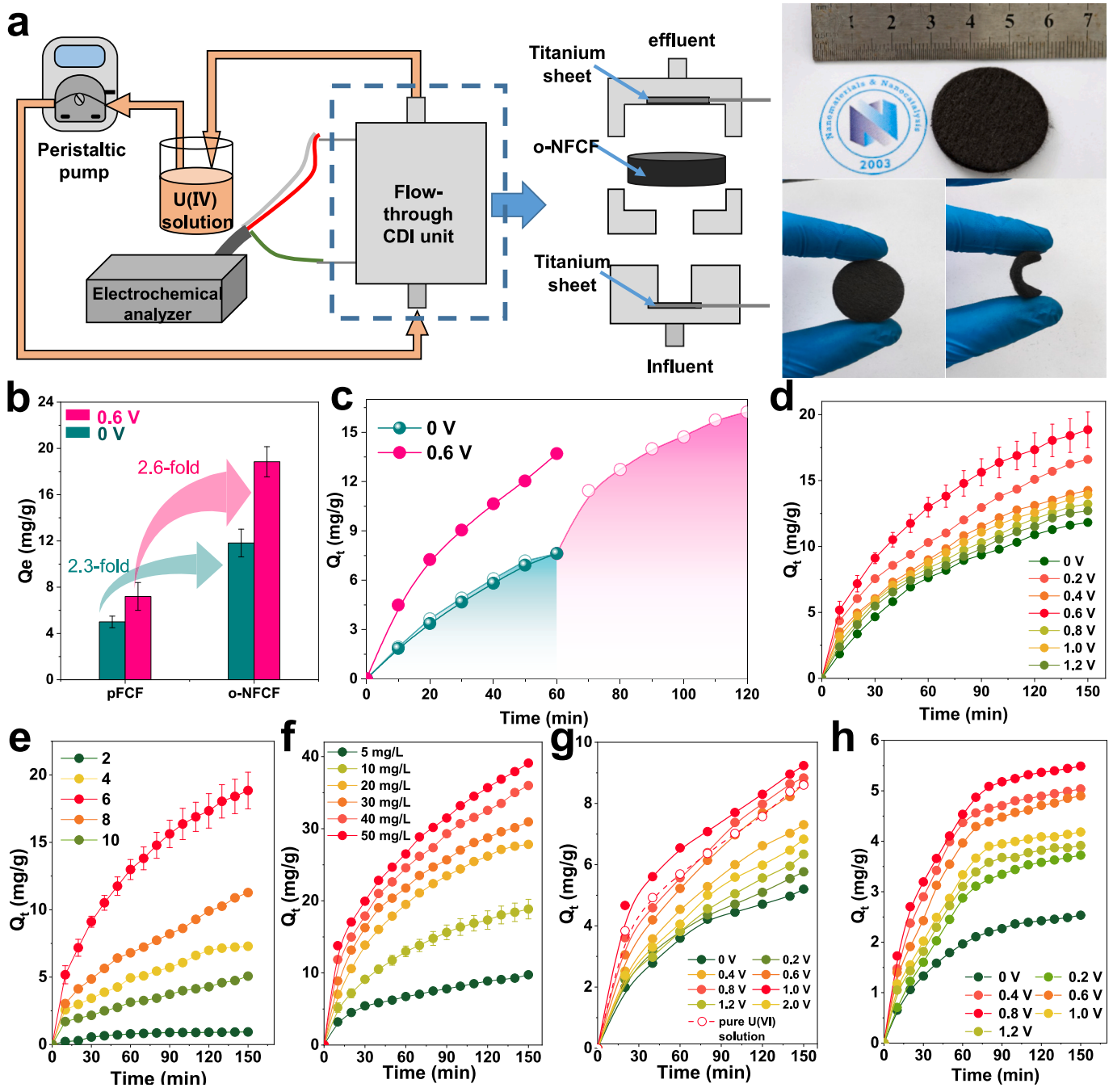

Fig. 2. (a) Schematic illustration of the electro adsorption of U(VI) with a Flow-through operation in the self-designed device. (b) The performance comparison of different adsorbents. (c) The adsorption enhancement under different operations. The influence of applied voltage (d), pH (e), initial concentration (f), applied voltage on the adsorption efficiency in the simulated seawater (g) and real seawater (h) over o-NFCF.

carbon material and U(VI) ions, thereby improving adsorption performance. To further highlight the significant role of the electric field, the adsorption of U(VI) over o-NFCF was initially carried out without an electric field, followed an enhancement of an electric field. When the adsorption capacity gradually reached the equilibrium after 60 min, an applied voltage of 0.6 V was introduced (Fig. 2c). The adsorption capacity was significantly enhanced and approached the high adsorption capability, which was close to that of direct electrosorption, indicating that an external electric field could further promote the adsorption of ions on the surface.

Based on the above findings, the effects of adsorption conditions (electric field strength, pH value, and initial concentration) were explored using o-NFCF as a typical adsorbent (Fig. 2d-f). In current study, the application of the electric field directly varied the electrostatic adsorption force between the adsorbent and metal ions to improve the adsorption capacity. Here, the influence of the electric field was studied by adjusting the applied voltage (0–1.2 V) (Fig. 2d). Without an external electric field (0 V), the adsorption capacity of the carbon adsorbent increased and approached equilibrium after 150 min (approximately 11.8 mg/g). Further introduction of an electric field with the variation of adsorption capacity over o-NFCF was observed with a volcanic tendency along with the increasing external voltage. The optimal adsorption performance of o-NFCF (18.8 mg/g at 150 min) was achieved at an applied voltage of 0.6 V. Analysis suggested that at low external voltages, the electrical driving force was insufficient, resulting in lower adsorption performance. Conversely, applying high voltages (>0.6 V)

led to energy wastage due to the possible electrochemical reactions, thereby weakening the adsorption performance for U(VI).

The pH value influenced the ionic forms, e.g., UO_2^{2+}, UO_2OH^+, $UO_2(OH)_2$, $(UO_2)_2(OH)_2^{2+}$, $(UO_2)_2OH^{3+}$, $(UO_2)_3(OH)^{2+}$, $(UO_2)_4(OH)^{7+}$, UO_2CO_3, $UO_2(CO_3)_2^{2-}$, and $UO_2(CO_3)_3^{4-}$, and the surface charge of the adsorbent as well [30]. These variations would significantly affect the adsorption behavior of an adsorbent. Under low-pH conditions (pH < 7), the main form of U(VI) in the aqueous solution was the stable and mobile uranyl ion (UO_2^{2+}). As the pH increased, UO_2^{2+} in aqueous solution tended to be hydrolyzed to form hydroxyl complexes such as $UO_2(OH)_x$. In fact, when the pH value of the aqueous solutions varied from 1 to 10, U(VI) primarily existed in the forms of UO_2^{2+}, $(UO_2)_2(OH)_2^{2+}$, $(UO_2)_3(OH)^{5+}$, and $(UO_2)_4(OH)^{7+}$. The influence of pH (2–10) on the U (VI) adsorption on o-NFCF was investigated (Fig. 2e). The results showed that when the pH value was <2, o-NFCF exhibited negligible adsorption capacity for U(VI), probably ascribed to the competition adsorption of H^+, H_3O^+ and UO_2^{2+} on the adsorbent surface. When the pH value was >4, the surface of the adsorbent gradually deprotonated, generating negative charges that attracted positively charged U(VI) species (i.e., $UO_2(OH)^+$, $(UO_2)_4(OH)^{7+}$, and $(UO_2)_3(OH)^{5+}$) to enhance the performance. Herein, the optimal adsorption performance was observed (18.8 mg/g) with a pH value of 6. As the pH continued to rise, the adsorption capacity began to decline, reaching only 11.2 mg/g (at 150 min) when the pH value was 10. Initial concentration strongly governed both the electrosorption kinetics and the ultimate recovery of U(VI). Experiments conducted at 5–50 mg/L revealed that o-NFCF capacity rose steadily with concentration (Fig. 2f), evidencing abundant accessible adsorption sites. Beyond 40 mg/L, however, the slope flattened, indicating that these sites were approaching saturation.

U(VI) extraction from seawater was an important approach for achieving high-yield U(VI) production. Seawater as the huge U(VI) resources could offer thousands of times the total terrestrial reserves [31]. Therefore, extracting U(VI) from seawater was significant for ensuring the sustainable development of nuclear energy. However, due to the challenges of poor U(VI) selectivity and high energy consumption in high-salinity environments [7], there was an urgent need to develop new adsorption and extraction technologies. Since the pH of seawater was between 7.3 and 8.3, under which conditions U(VI) formed stable [$UO_2(CO_3)_3^{4-}$] (aq) complexes [32], it could be inferred from the aforementioned results that o-NFCF could still effectively electrosorb U (VI) from the real seawater. Considering that the concentration of U(VI) in real seawater was extremely low, to meet the detection limit in the laboratory, the studies were subsequently conducted by adding U(VI) ions into the solution with an U(VI) concentration of 10 mg/g. The ability of o-NFCF to adsorb U(VI) ions in simulated seawater was investigated [33] (Fig. 2g). As the significant increase of ion concentration in the simulated seawater would definitely alter the conductivity of the solution, the influence of the applied voltage on U(VI) adsorption capacity with an initial U(VI) concentration of 10 mg/L in the simulated seawater was explored. At an applied voltage of 1.0 V, the optimized adsorption capacity was 9.2 mg/g, showing a decreased activity (lower than that in pure U(VI) solution). Notably, the adsorption activity in the simulated seawater at 1.0 V was slightly higher than that in pure U(VI) solution (8.5 mg/g at 1.0 V in Fig. 2d), probably ascribed to the increased ion concentration in the solution, which enhanced the solution conductivity and the electrosorption capability.

However, real seawater was found to contain not only high concentrations of sea salt ions such as K^+, Ca^{2+}, Na^+, and Mg^{2+}, which competed with U(VI) for adsorption sites, but also a large number of marine organisms, including microbes, bacteria, algae, and animals. The biofouling caused by these organisms severely limited the adsorption performance and durability of the material [34]. Consequently, the adsorption performance of o-NFCF in real seawater containing 10 mg/L of U(VI) (pH = 7.42) was further investigated (Fig. 2h). Although the electric field significantly impacted the performance of o-NFCF, the optimal adsorption capacity in seawater was found to be 7.7 mg/g at 0.8 V, which was lower than those in simulated seawater and pure solution. This reduced activity might be caused via the formation of a thin organic film on the adsorbent by microbes and bacteria, which inactivated and blocked some of the active sites [35,36]. Herein, the adsorption process was influenced by the concentration of ions and the existence of microbes and bacteria. Notably, in the real seawater, the adsorption equilibrium was nearly reached within 70 min, significantly reducing the operation time. The ion selectivity over abundant seawater cations (N^{a+}, Mg^{2+}, and Ca^{2+}) was also the key parameter. In this work, we also evaluated the ion selectivity during the electro adsorption process (Fig. S3). The result demonstrated that the adsorption capacities (*Qe*) of Na^+, Mg^{2+}, and Ca^{2+} ions over the o-NFCF under a voltage of 0.6 V were 0.5, 0.9, and 1.0 mg/g, respectively, which were much lower than that of U(VI) (7.7 mg/g). The significant performance difference indicated that the developed strategy in this work exhibited high selectivity in extracting U(VI) ions from the real seawater.

Furthermore, the energy consumption per gram of extracted uranium ($E_{U(VI)}$) is fully discussed (Fig. S4). During the electro adsorption of U (VI) in the pure solution, the value of $E_{U(VI),\ pure\ solution}$ slightly increased from 0.08 to 1.39 Wh/g. For the simulated seawater and real seawater, the value of $E_{U(VI),\ simulated\ seawater}$ and $E_{U(VI),\ real\ seawater}$ were much higher than that of $E_{U(VI),\ pure\ solution}$, probably ascribed to the high concentration of ions, which might induced the faradic reactions, e.g. the hydrogen evolution reaction [37,38]. Meanwhile, the value of $E_{U(VI),\ simulated\ seawater}$ was close to that of $E_{U(VI),\ real\ seawater}$, showing that the presence of microorganisms would not greatly influence the energy consumption. Meanwhile, we found that the $E_{U(VI),\ real\ seawater}$ was calculated to be 13.9 Wh/g at 0.8 V, which was higher than the electrochemical uranium extraction (EUE) technique developed by Wang et al. (0.5 Wh/g) [4], but lower than the traditional EUE system (517.2 Wh/g), showing the potential for the practical application.

The study of adsorption kinetics helped us understand the interactions between the adsorbents and ions in the adsorption process. In this research, the adsorption kinetics of o-NFCF were investigated in pure U(VI) solution, simulated seawater, and real seawater. To elucidate the adsorption behavior over o-NFCF towards U(VI), two models i.e., pseudo-first-order and pseudo-second-order kinetic models, were utilized (Fig. 3a and b) [39], and the calculation results were summarized (Table S1). Regardless of whether the electric field was 0 V or 0.6 V, the pseudo-first-order model did not fit the experimental data well, with R^2 values of 0.914 and 0.954, respectively. In contrast, the experimental was well fitted by the pseudo-second-order model, with correlation coefficients of 0.998 at 0 V and 0.991 at 0.6 V, indicating that the adsorption of U(VI) ions by o-NFCF followed the pseudo-second-order model, suggesting that chemisorption dominated the entire adsorption process.

To further investigate the adsorption mechanism, the Langmuir and Freundlich isotherms were employed to study the adsorption behavior of o-NFCF towards U(VI) ions (Fig. 3c-f). It was observed that both the 0 V and 0.6 V systems, the R^2 values obtained from the Langmuir isotherm fitting (0.98 and 0.995) were higher than those from the Freundlich isotherm (0.939 and 0.96) (Table S2). These results indicated that the monolayer adsorption on the surface of o-NFCF was confirmed, where the adsorption sites had uniform energy and formed a homogeneous monolayer coverage. Comparing the three different solution systems (pure U(VI) solution, simulated seawater, and real seawater), the presence of an electric field significantly enhanced the adsorption capacity of the FCF material. However, the maximum adsorption capacity decreased progressively in the simulated seawater and real seawater, due to the influence of ions (i.e., Na^+, Mg^{2+}, Cl^-, CO_3^{2-}, HCO_3^- etc.) and pollutants (i.e., bacteria, microorganism etc.). The order of maximum adsorption capacities under electric field enhancement was as follows: $Q_{max,\ pure\ U(VI)\ solution}$ (44.6 mg/g) > $Q_{max,\ simulated\ seawater}$ (16.4 mg/g) > $Q_{max,\ real\ seawater}$ (10.6 mg/g). The Freundlich isotherm fitting analysis revealed that in all three solution systems, with or without an electric field. The order of K_f value was as follows: $K_{f,\ pure\ water}$ > $K_{f,\ simulated}$

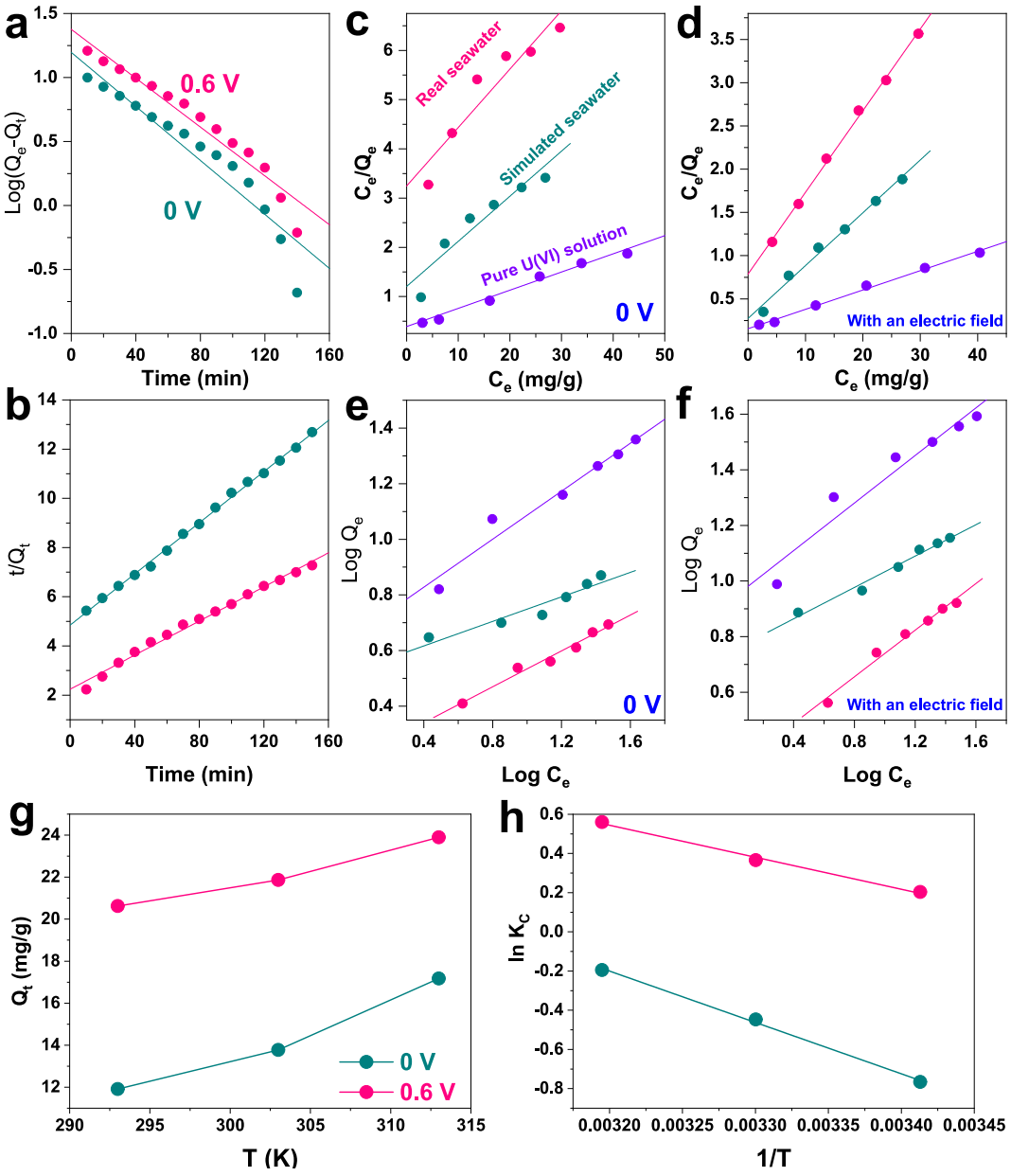

Fig. 3. U(VI) electro-adsorption on o-NFCF was kinetically described by (a) pseudo-first-order and (b) pseudo-second-order models. Equilibrium data were analyzed with Langmuir (c, d) and Freundlich (e, f) isotherms in the presence and absence of an electric field for different solutions. (g) Temperature dependence of U(VI) uptake on o-NFCF and (h) corresponding van't Hoff plots of ln K versus 1/T, with and without applied voltage.

$_{\text{seawater}} > K_{\text{f, Real seawater}}$, indirectly confirming that the o-NFCF more readily adsorbed U(VI) ions in the pure water system. The values of n were all greater than 1, indicating that the adsorption process was more favorable for low-concentration solutions. The aforementioned test results demonstrated that an electric field could enhance the adsorption of U(VI) by o-NFCF from water, and it was feasible to improve the carbon material's adsorption performance for U(VI) by applying an electric field.

Moreover, a comparison of adsorption capacity, enrichment factor, stability, and cycle performance with recent adsorbents (amidoxime-based polymers, MOFs, carbon-based materials) was conducted (Table S3). And we found that the Q_{max} of o-NFCF was 44.6 mg/g, higher than the typical carbon adsorbents (3.4 mg/g of AC, 3.8 mg/g of ACF, and 2.1 mg/g of activated carbons) [40–42], but lower than the MOF-based materials (410.3 mg/g of N-doped MOF-199 and 375.5 mg/g of UiO-66/GO) and some amidoxime-based polymers-based materials-based materials (379 mg/g of polyguanidine-modified amidoxime-based fiber) [9,43,44]. Meanwhile, the comparably low enrichment factor of o-NFCF (3.2) was observed. It was close to other carbon adsorbents (3.2 of AC, 5.8 of activated carbons) [40,42], while, lower than that of MOF-based materials (21.7 of N-doped MOF-199 and 19.0 of UiO-66/GO) and some amidoxime-based polymers-based materials-based materials (13.3 of amidoxime-modified poly(vinyl alcohol) fiber and 15.9 of amidoxime-modified mesoporous polymer microsphere) [9,43,45,46]. Therefore, our future study is to improve the enrichment factor and Q_{max} in the electro adsorption process.

Thermodynamic features of U(VI) electro-adsorption onto o-NFCF were assessed (Fig. 3g and h). Between 293 and 313 K, the uptake of U (VI) rose steadily with temperature. Standard enthalpy (ΔH°), Gibbs free-energy (ΔG°) and entropy (ΔS°) changes were derived from Eqs. S1–S3, which were listed in Table S4 [22,47]. In the absence of an electric field, positive ΔG° values revealed a non-spontaneous process that demands external energy. Upon application of 0.6 V, ΔG° became negative, signifying spontaneous adsorption that is increasingly favored

at higher temperatures. Positive ΔH° under both settings confirms the endothermic nature of the interaction; the value drops from 14.18 kJ/mol (0 V) to 11.61 kJ/mol (0.6 V), evidencing that the electric field strengthens U(VI)–o-NFCF affinity and lowers the energy barrier. The positive ΔS° further indicates greater disorder at the solid–liquid interface upon U(VI) uptake.

3.3. Recyclability test

The recyclability of the adsorbent was also a key factor in determining its potential for industrial application. Fig. 4a illustrates the changes in the adsorption capacity of U(VI) by the o-NFCF electrode during multiple consecutive regeneration cycles in real seawater. The electrode was regenerated on the original adsorption apparatus by reversing the electrodes and passing 400 mL of 0.1 mol/L Na_2SO_4 solution at 80–90 °C unidirectionally through the electrosorption unit, with sodium sulfate used as an electrolyte to enhance the solution's conductivity. It was observed that without the application of an electric field during adsorption and desorption, the adsorption performance was poor and rapidly deteriorated, indicating that a large number of U(VI) ions on

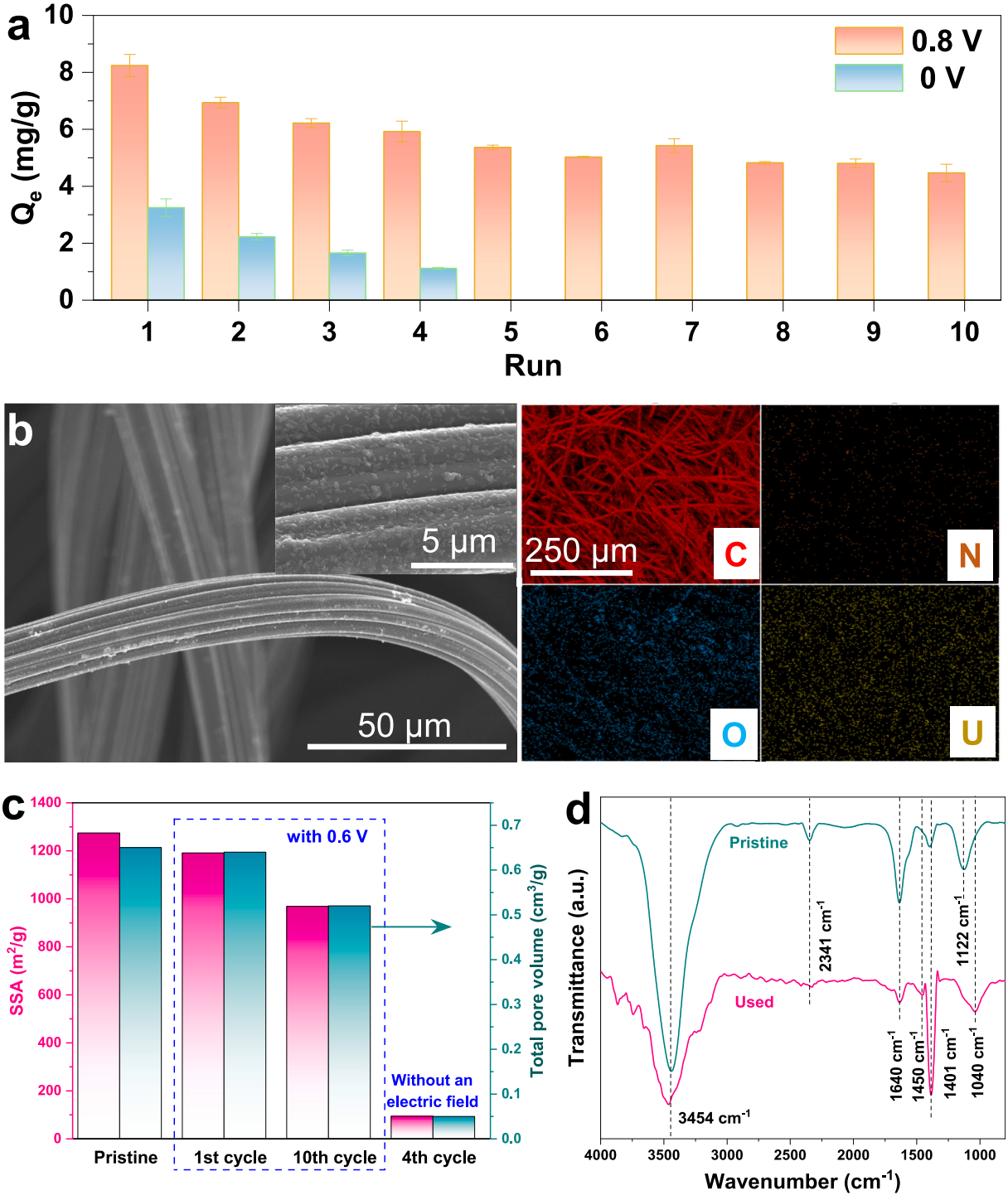

Fig. 4. (a) Comparison of the stability over carbon adsorbent in the real seawater with and without an electric field. (b) SEM and EDS images, (c) variation of SSA during the cycles and (d) FT-IR spectrum of the pristine and used o-NFCF.

the material's surface could not be effectively desorbed and might have been blocked by microorganisms in the real seawater. When an electric field of 0.8 V was applied during adsorption and 1.5 V during desorption (with reversed electrodes), the regeneration performance of the carbon adsorbent still decreased in the first five cycles, likely due to some micropores in o-NFCF being blocked by adsorbed ions, ultimately reducing the desorption efficiency. However, after the sixth cycle, the performance stabilized, with an adsorption capacity of 4.5 mg/g after 10 cycles, which was still 54 % of the initial adsorption capacity, demonstrating the considerable stability.

A series of characterizations were carried out on the o-NFCF material after adsorption (Fig. 4b–e). The SEM image showed that the fiber arrangement became disordered, and more nanoparticles on surface were observed (Fig. 4b). The elemental distribution map indicated that U elements were uniformly distributed on the surface of the o-NFCF material (Fig. 4c). The specific surface area (SSA) of o-NFCF decreased from 1258.5 m^2/g to 1191.2 m^2/g after the first adsorption, and the pore volume decreased from 0.68 cm^3/g to 0.64 cm^3/g (Figs. 4d and S5). Meanwhile, after 10 cycles with an electric field, the SSA remained at 968.9 m^2/g, whereas after four cycles without an electric field, the SSA was only 94.3 m^2/g, with a significant decrease in pore volume at the same time. This clearly indicated that the reversed applied voltage would accelerate the desorption of U(VI) ions from the inside pores of o-NFCF, which was the key factor for the regeneration of carbon adsorbent. When the adsorption/desorption processes were conducted without an electric field, a large number of ions were not desorbed and blocked the nano pores inside the o-NFCF, which was the fundamental reason for the sharply decrease of the stability. The FT-IR results indicated a reduction in the number of -OH groups on the carbon surface and a significant increase in -COOH groups (Fig. 4e) [28]. This suggested that -OH groups may have coordinated with U(VI) ions. The new peaks at 1450 cm^{-1} and 1040 cm^{-1} corresponded to carboxylate and alkoxy groups, respectively [48], indicating that oxidation occurred on the carbon surface during the electrosorption process.

It was believed that the formation of marine biofouling on the electrode surface is a developmental process, which involves the adsorption of organic molecules, attachment of bacterial cells, formation of a dense microbial biofilm et al. [49–51]. This biofouling is the critical barrier for seawater extraction technologies. Herein, excluding the effect of biofouling is the significant issue for the U(VI) extraction from seawater. In this study, 0.12 g o-NFCF was immersed into 4 L real seawater for 5 days, which contained 800 μL GY-H2IZ. The results demonstrated that there was no apparent change of the activity during the cycles (Fig. S6). This phenomenal indicated that the electro adsorption of U(VI) via a flow-through model from real seawater would not be affected by the biofouling.

3.4. Enrichment of U(VI) from the real seawater

The aforementioned results demonstrated that the o-NFCF adsorbent could achieve in-situ regeneration through the efficient desorption of surface ions via the reversed applied voltage. Herein, we attempted to follow this strategy to extract and enrich U(VI) ions from real seawater for effective recovery. In this process, each adsorption cycle utilized 1 L of real seawater solution with an initial U(VI) concentration of 1 mg/L (pH = 7.76). After adsorption, the U(VI) ions on the surface of the carbon material were electrochemically desorbed into a fixed 100 mL solution, thereby enriching the U(VI) ions. As shown in Fig. 5, the concentration of the enriched solution gradually increased with each consecutive extraction cycle. After eight cycles, the concentration reached 5.85 mg/L, which was higher than that of the initial adsorption solution. Meanwhile, the increased concentration of Na^+ was also evaluated and displayed a comparably lower amount of Na^+ ions from real seawater was enriched in the solution, even though the concentration of Na^+ was much higher than that of U(VI) in the initial solution. This clearly demonstrated that the electrosorption and enrichment of U (VI) by the o-NFCF material was a promising method for selectively extracting U(VI) from the real seawater, showing the practical potential for large-scale recovery.

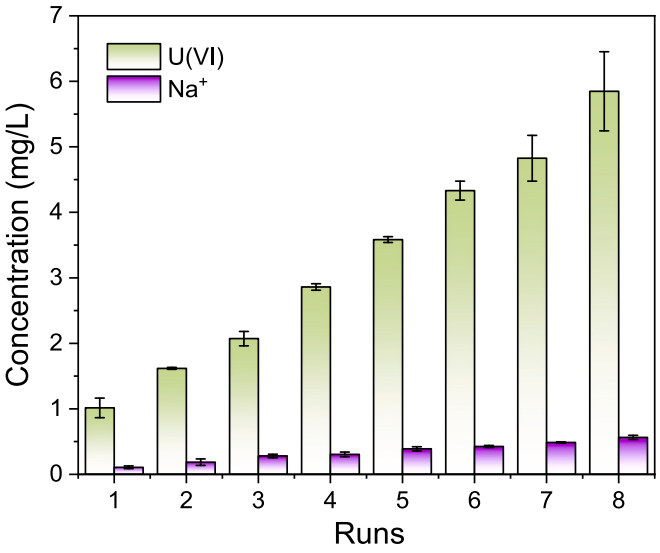

Fig. 5. The enrichment of U(VI) ions over o-NFCF aided with an electric field.

3.5. Mechanism study

To reveal the reasons behind the superior performance and the underlying mechanisms of electrosorption, the substantial effects of material surface properties on adsorption performance were carefully analyzed. In the field of electro adsorption of metal ions over carbon-based adsorbents from aqueous solutions, numerous reports highlighted the dominant role of N atoms and oxygen functionalities of carbon adsorbents in the adsorption of metal ions [21,22,35,52]. Our previous work also revealed that the synergistic effect of N atoms and oxygen functionalities would enhance the adsorption performance of carbon materials towards Pt(VI) [22]. Therefore, in this work, the impact of the nitrogen-to-oxygen ratio (N/O) on the surface of carbon materials on their electrosorption capacity of U(VI) was investigated, to reveal the significant role of surface properties. The o-NFCFs materials with different contents of N and O elements were prepared (Table S5). As shown in Fig. 6c, the electrosorption capacity of p-FCF and the o-NFCF series materials exhibited an inverted volcanic tendency along with the variation of N/O ratio. This indicated that N atoms and oxygen functional groups on the surface of carbon materials, as key adsorption sites, could effectively regulate the electrosorption capacity, but their ratio had to be within a reasonable range to enhance adsorption activity effectively. Also, the relationship between the N/O doping and uranyl carbonate species adsorption in seawater conditions was investigated (**Fig. S7**). The results showed that the electrosorption capacity of FCFs materials demonstrated a firstly decrease and then increase activity, which was similar to that in pure solution. However, it remained unclear how N and O elements worked together to improve the electrosorption performance of materials, and further research was needed to uncover the essential reasons behind their influence on adsorption performance.

The DFT simulations were then carried out to reveal the synergistic effect of N dopants and oxygen-containing groups on the adsorption behavior. Here, we utilized graphene (G), graphene with -containing group (O/G), N doped graphene (N/G), N doped graphene with -containing group (NO/G), and UO_2^{2+} ion as the model substrates to investigate the role of different functionalities on the adsorption of U(VI) process (Fig. 6d). The adsorption energies (E_a) for these optimized configuration were obtained. The results demonstrated that $E_{a,G-UO_2^{2+}}$ was calculated to be −3.24 eV, indicating that the carbon materials

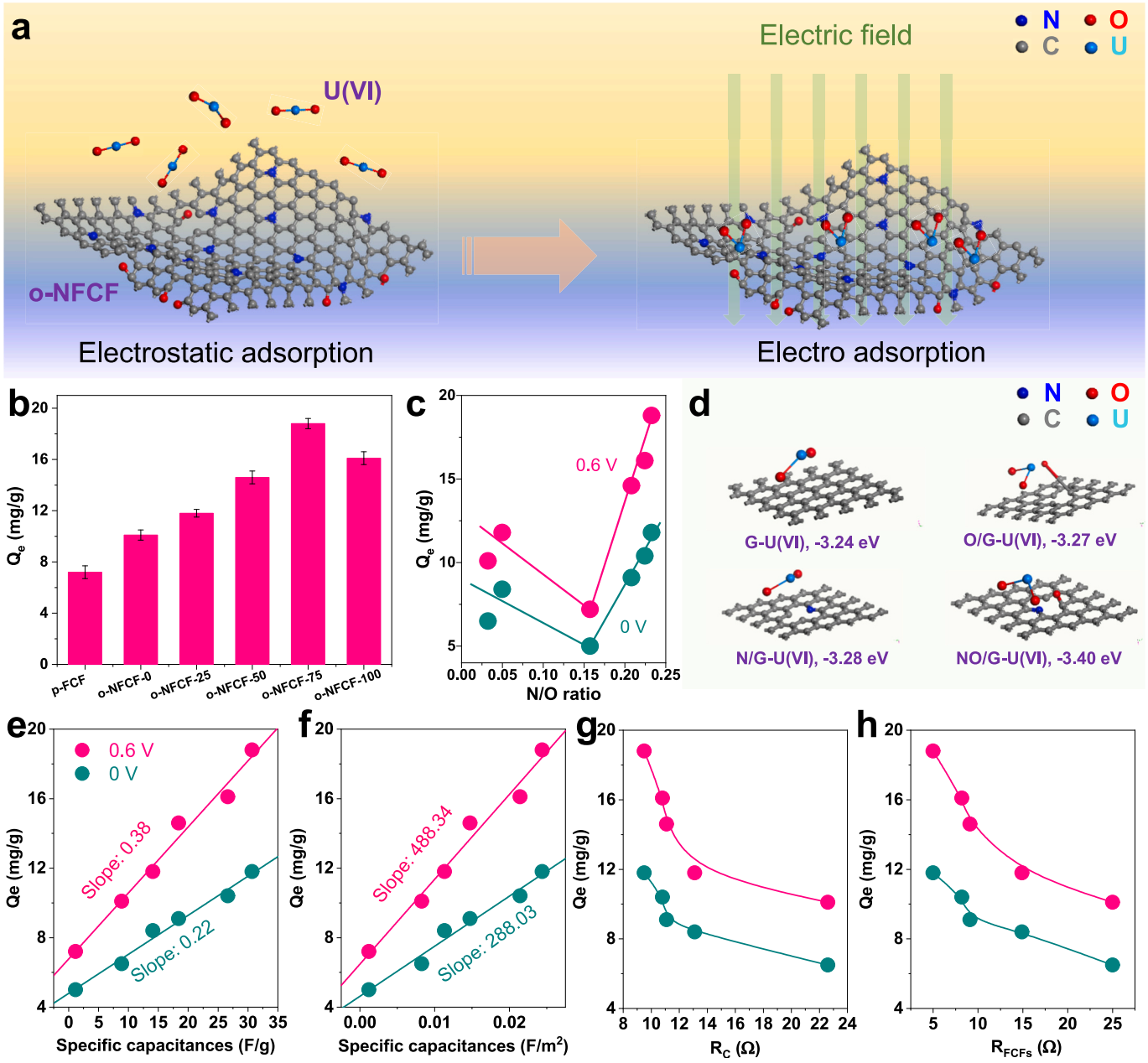

Fig. 6. (a) Conceptual diagrams comparing electro-adsorption (field-driven ion migration) and electrostatic adsorption (surface charge-based capture). (b) U(VI) uptake of carbon adsorbents under applied electric fields. (c) Dependence of equilibrium capacity (Q_e) on the N/O ratio at 0 and 0.6 V in the pure solution. (d) DFT-calculated adsorption energies of U(VI) on carbon surfaces. (e, f) Dependence of Q_e on the capacity normalized by mass and by surface area at 0 and 0.6 V in the pure solution. (g, h) Dependence of Q_e on the residual carbon (R_C) and relative fluorinated carbon fragments (R_{FCFs}) at 0 and 0.6 V in the pure solution.

could be used as the adsorbent for the adsorption of U(VI) ions [7,53]. The introduction of N dopant or oxygen-containing groups on the surface would strengthen the interactions between carbon adsorbent and U (VI), in which $E_{a,N/G-UO_2^{2+}}$ and $E_{a,O/G-UO_2^{2+}}$ were calculated to be −3.28 and − 3.27 eV, respectively. Moreover, this interaction could be further enhanced by the coexistence of N doping and oxygen-containing groups on the surface of carbon adsorbent with a $E_{a,O/G-UO_2^{2+}}$ of −3.40 eV. These results demonstrated that the surface modification (i.e., heteroatoms doping and oxygen-containing groups etc.) could act as the key sites and dominate the adsorption process [53].

The electrochemical properties of carbon materials typically demonstrated a significant impact on the electrosorption process as well [22]. In this study, electrochemical tests were carried out on p-FCF and the o-NFCF series materials (Figs. S8–S9 and Table S5). The cyclic voltammetry (CV) test of FCFs showed that the lowest the specific capacitance of pFCF (1.18 F/g and 0.0012 F/m^2) was observed. Meanwhile, the surface modified o-NFCFs materials displayed the improved specific capacitance, which firstly increased and then decreased alongside with the increase of the formamide concentration in the solvothermal process. The o-NFCF-75 showed the highest specific capacitance (30.7 F/g and 0.0243 F/m^2). The electrochemical impedances of these materials were evaluated as well. And the results demonstrated that the suitable modification of FCFs would efficiently reduce the impedance of carbon material, in which o-NFCF-75 displayed the lowest electrochemical impedance (R_C and R_{FCFs} were tested as 9.5 Ω and 5.0 Ω, respectively.). These results indicated that in this experiment, the capacitive performance and resistance values of pFCFs in U(VI) solution were both influenced by the synergistic effect of surface N and O content.

The relationship between specific capacitance and resistance with electrosorption capacity was then established. As shown in Fig. 6e–f, both specific capacitance per unit mass or area and adsorption capacity exhibited a linear positive correlation, further confirming that the capacitive performance of 3D-FCF materials played a dominant role in the adsorption of U(VI) ions, and carbon materials with higher capacitance showed greater electrosorption capacity. Additionally, a similar trend was observed in the relationship between resistance and adsorption capacity (Fig. 6g–h). When $R_C < 19.9\ \Omega$ and $R_{o\text{-}NFCFs} < 14.9\ \Omega$, carbon materials with lower resistance exhibited higher electrosorption capacity. This was because when the resistance was lower, the electric field was more widely distributed on the surface of the carbon felt, thereby enhancing the adsorption performance. The above discussion fully demonstrated that the electrochemical properties of 3D-FCF materials played a dominant role in their electrosorption capacity for the radioactive metal U(VI).

4. Conclusions

In summary, pFCF and o-NFCF as the adsorbents for the electro adsorption and enrichment of U(VI) via a Flow-through operation in the laboratory-designed device was developed. Under the conditions of an initial concentration of 10 mg/L, 0.6 V, and pH = 6, o-NFCF demonstrated the best electrosorption performance with a Q_e reaching 18.8 mg/g, higher than that without an electric field (11.8 mg/g, 0 V) and the pFCF system (7.2 mg/g, 0.6 V). The Q_{max} of o-NFCF in pure U(VI) solution was 44.6 mg/g, comparable to the traditional adsorbents. The electro adsorption performances of U(VI) were also conducted in the simulated and real seawater, displaying the decreased Q_e at their optimized conditions (9.24 mg/g at 1.0 V for simulated seawater and 7.7 mg/g at 0.8 V for real seawater, respectively) with the considerable Q_{max} (16.4 mg/g for simulated seawater and 10.6 mg/g for real seawater, respectively). This decreased activity revealed that the complex environment and challenge for the uptake of U(VI) from real seawater. Moreover, the o-NFCF material maintained an acceptable stability after 10 cycles in real seawater in the presence of an electric field, which led to the realization of the enrichment of U(VI) from the real seawater. In-depth mechanistic studies and DFT simulations revealed that the ratio of N/O on the surface of the carbon material might regulate the activity of o-NFCFs, while their electrochemical properties were found to more important to promote the electrosorption performance. This investigation offers a potential method for extracting and enrichment of U(VI) from the real seawater.

CRediT authorship contribution statement

Jiangnan Huang: Writing – original draft, Resources, Investigation, Data curation. **Shuang Chen:** Writing – original draft, Methodology, Investigation, Data curation. **Yingjie Ruan:** Investigation, Data curation. **Hao-Fan Wang:** Validation, Resources, Methodology. **Hongjuan Wang:** Validation, Resources, Methodology. **Hao Yu:** Validation, Resources, Methodology. **Yonghai Cao:** Writing – review & editing, Supervision, Resources, Project administration, Methodology, Investigation.

Declaration of competing interest

The authors declare that they have no known competing financial interests or personal relationships that could have appeared to influence the work reported in this paper.

Acknowledgements

We would like to acknowledge the financial support from the National Natural Science Foundation of China (22272056), Guangdong Basic and Applied Basic Research Foundation (2022A1515140108), CNPC Innovation Found (2021DQ02-0704), Research Fund Program of Guangdong Provincial Key Laboratory of Fuel Cell Technology (FC202305), and the start-up fund from Zhongkai College of Agricultural Engineering.

Appendix A. Supplementary data

Supplementary data to this article can be found online at https://doi.org/10.1016/j.seppur.2025.135353.

Data availability

Data will be made available on request.

References

[1] A.E. Geweda, M.E. Zayed, M.Y. Khan, A.B.S. Alquaity, Mitigating CO_2 emissions: a review on emerging technologies/strategies for CO_2 capture, J. Energy Inst. 118 (2025) 101911.
[2] C. Zhang, M.G. Rahman Zafar, F. Gaudreault, O. Ben-Salha, A. Alhebri, Stringent environmental policies: how they shape the future of nuclear energy generation, Nucl. Eng. Technol. 57 (2025) 103650.
[3] S. Yang, Z. Ye, X. Cheng, Y. Wang, Z. Luan, W. Li, B. Hu, Electro-adsorption and reduction of uranium(VI) by Fe3O4@COFs electrode with enhanced removal performance, Chem. Eng. J. 474 (2023) 145598.
[4] Y. Wang, G. Wen, Z. Liu, T.T. Thuy Nga, C.-L. Dong, J. You, C. Xie, S. Du, F. Zhang, Q. Liu, J. Wei, Y. Cao, X. Peng, Y. Yuan, Y. Wang, S. Wang, Bipolar electrochemical uranium extraction from seawater with ultra-low cell voltage, Nature Sustain. 8 (2025) 682–691.
[5] Y. Zhang, Y. Wang, Z. Dong, Y. Wang, Y. Liu, X. Cao, Z. Zhang, C. Xu, N. Wang, Y. Liu, Boosting uranium extraction from seawater by micro-redox reactors anchored in a seaweed-like adsorbent, Nat. Commun. 15 (2024) 9124.
[6] M. Huang, L. Xie, Y. Wang, H. He, H. Yu, J. Cui, X. Feng, Z. Lou, Y. Xiong, Efficient uranium electrochemical deposition with a functional phytic acid-doped polyaniline/graphite sheet electrode by adsorption-electrodeposition strategy, Chem. Eng. J. 457 (2023) 141221.
[7] C.W. Abney, R.T. Mayes, T. Saito, S. Dai, Materials for the recovery of uranium from seawater, Chem. Rev. 117 (2017) 13935–14013.
[8] K. Wan, S. Yuan, J. Zhang, Y. Shen, M. Zhao, K. Yan, Z. Wang, Enhanced seawater uranium extraction via flow capacitive deionization by amidoxime-functionalized MXene/CoZn-MOF heterostructure electrodes, Water Res. 285 (2025) 124149.
[9] Q. Hu, D. Wang, J. Liang, Z. Liu, J. Li, Porous carbonized N-doped MOF-199 modified with MWCNTs for the deionization of uranium(VI), Sep. Purif. Technol. 330 (2024) 125494.
[10] Z. Wang, Q. Meng, R. Ma, Z. Wang, Y. Yang, H. Sha, X. Ma, X. Ruan, X. Zou, Y. Yuan, G. Zhu, Constructing an ion pathway for uranium extraction from seawater, Chem 6 (2020) 1683–1691.
[11] Q. Ren, Y. Wang, Y. Wang, Z. Feng, Y. Du, C. Wang, Y. Liu, D. Yuan, H. Jiang, Y. Li, Inspiring the potential of graphene oxide aerogel for uranium(VI) electrosorption: a precursor reconfiguration strategy and synergistic integration with polyethyleneimine, Desalination 609 (2025) 118883.
[12] H. Guo, E. Hu, Y. Wang, Z. Ou, B. Huang, J. Lei, H. Liu, R. He, W. Zhu, A synergistic coordination-reduction interface for electrochemical reductive extraction of uranium with low impurities from seawater, Nat. Commun. 16 (2025) 2012.
[13] T. Li, Z. Yan, S. Chen, Y. Song, X. Lin, Z. Zhang, L. Yang, X. He, Y. Qian, S. Zhou, X. Li, Q. Wang, X.Y. Kong, L. Jiang, L. Wen, Heart trabeculae-inspired superhydrophilic electrode for electric-assisted uranium extraction from seawater, Adv. Funct. Mater. 35 (2024) 2412349.
[14] C. Zhang, Z. Wang, R. Ma, J. Cao, X. Ruan, D. Cao, Y. Song, S. Chen, Y. Song, F. Wang, Y. Yuan, Y. Yang, G. Zhu, Overcoming chemical dissociation processes: electrochemical modulation of high-affinity binding sites for rapid uranium extraction from seawater, Adv. Funct. Mater. 35 (2024) 2412712.
[15] J. Chen, J. Gao, Y. Liu, H. Lv, J. Han, Y. Yan, F. Ma, Q. Chen, Y. Xue, Anode-assisted enhanced electrosorption for efficient uranium removal at ultra-low cell voltage, Chem. Eng. J. 507 (2025) 160421.
[16] H. Ye, T.-H. Li, Y.-Q. Huang, J.-M. Jin, J.-Y. Fei, M.-B. Wu, J. Yao, Amyloid-like coatings decorated electrodes boost the uranium electro-adsorption from seawater, Chem. Eng. J. 451 (2023) 138615.
[17] H. Liu, G. Tian, W. Wang, J. Zhang, T. Wu, X. Ni, Y.-H. Wu, Carbon fiber-based flow-through electrode system (FES) for Cr(VI) removal at near neutral pHs via Cr (VI) reduction and in-situ adsorption of Cr (III) precipitates, Chem. Eng. J. 420 (2021) 127622.
[18] Y. Wang, J. Zhang, W. Wang, T. Wu, Y. Sun, H. Wu, D. Chen, H. Liu, Enhancement of Cr(VI) reduction by polyaniline nanorod-modified cathode in flow-through electrode system, Chem. Eng. J. 429 (2022) 132553.
[19] Y. Liu, Y. Zhang, Y. Zhang, Q. Zhang, X. Gao, X. Dou, H. Zhu, X. Yuan, L. Pan, MoC nanoparticle-embedded carbon nanofiber aerogels as flow-through electrodes for highly efficient pseudocapacitive deionization, J Mater Chem A 8 (2020) 1443–1450.

[20] Y.-U. Shin, W. Pan, S.K. Patel, J. Lim, L.R. Winter, W. Ma, S. Hong, M. Elimelech, Electrochemical chromium removal using nanodiamond enhanced flow-through electrosorption, Chem. Eng. J. 474 (2023) 145756.
[21] B. Wang, Q. Jiang, G. Yang, H. Wang, H. Wang, F. Peng, H. Yu, J. Huang, G. Zhong, Y. Cao, Electric field-assisted uptake of hexavalent chromium ions with in situ regeneration of carbon monolith adsorbents, Adv. Sci. 10 (2023) 2301419.
[22] S. Chen, K. Huang, H.-F. Wang, H. Wang, H. Yu, J. Huang, Y. Cao, Electric-field enhanced three-dimensional flexible carbon felt as a host for Pt^{4+} ions extraction, Chem. Eng. J. 490 (2024) 151835.
[23] M. Jiang, J. Huang, G. Yang, H. Wang, H.-F. Wang, F. Peng, Y. Cao, H. Yu, In-situ regeneration of carbon monoliths as an environmental-benign adsorbent for environmental remediation via a flow-through model, Sep. Purif. Technol. 314 (2023) 123542.
[24] P. Hohenberg, W. Kohn, Inhomogeneous electron gas, Phys. Rev. 136 (1964) B864–B871.
[25] B. Delley, From molecules to solids with the DMol(3) approach, J. Chem. Phys. 113 (2000) 7756–7764.
[26] J.P. Perdew, K. Burke, M. Ernzerhof, Generalized gradient approximation made simple, Phys. Rev. Lett. 77 (1996) 3865–3868.
[27] S. Grimme, J. Antony, S. Ehrlich, H. Krieg, A consistent and accurate ab initio parametrization of density functional dispersion correction (DFT-D) for the 94 elements H-Pu, J. Chem. Phys. 132 (2010) 154104.
[28] A. Dandekar, R. Baker, M. Vannice, Characterization of activated carbon, graphitized carbon fibers and synthetic diamond powder using TPD and DRIFTS, Carbon 36 (1998) 1821–1831.
[29] D. Guo, Y. Liu, H. Ji, C.-C. Wang, B. Chen, C. Shen, F. Li, Y. Wang, P. Lu, W. Liu, Silicate-enhanced heterogeneous flow-through electro-Fenton system using iron oxides under nanoconfinement, Environ. Sci. Technol. 55 (2021) 4045–4053.
[30] F. Endrizzi, C.J. Leggett, L. Rao, Scientific basis for efficient extraction of uranium from seawater. I: understanding the chemical speciation of uranium under seawater conditions, Ind. Eng. Chem. Res. 55 (2016) 4249–4256.
[31] D. Shao, Y. Li, X. Wang, S. Hu, J. Wen, J. Xiong, A.M. Asiri, H.M. Marwani, Phosphate-functionalized polyethylene with high adsorption of uranium(VI), ACS Omega 2 (2017) 3267–3275.
[32] F. Endrizzi, L. Rao, Chemical speciation of uranium(VI) in marine environments: complexation of calcium and magnesium ions with $[(UO_2)(CO_3)_3]^{4-}$ and the effect on the extraction of uranium from seawater, Chem. A Eur. J. 20 (2014) 14499–14506.
[33] Y. Yuan, Q. Yu, M. Cao, L. Feng, S. Feng, T. Liu, T. Feng, B. Yan, Z. Guo, N. Wang, Selective extraction of uranium from seawater with biofouling-resistant polymeric peptide, Nature Sustain. 4 (2021) 708–714.
[34] Z. Huang, H. Dong, N. Yang, H. Li, N. He, X. Lu, J. Wen, X. Wang, Bifunctional phosphorylcholine-modified adsorbent with enhanced selectivity and antibacterial property for recovering uranium from seawater, ACS Appl. Mater. Interfaces 12 (2020) 16959–16968.
[35] J. Huang, Y. Li, Y. Cao, F. Peng, Y. Cao, Q. Shao, H. Liu, Z. Guo, Hexavalent chromium removal over magnetic carbon nanoadsorbents: synergistic effect of fluorine and nitrogen co-doping, J Mater Chem A 6 (2018) 13062–13074.
[36] D. Zhao, W.Y. Cheah, S.H. Lai, E.-P. Ng, K.S. Khoo, P.L. Show, T.C. Ling, Symbiosis of microalgae and bacteria consortium for heavy metal remediation in wastewater, J. Environ. Chem. Eng. 11 (2023) 109943.
[37] L. Zhou, D. Guo, L. Wu, Z. Guan, C. Zou, H. Jin, G. Fang, X.A. Chen, S. Wang, A restricted dynamic surface self-reconstruction toward high-performance of direct seawater oxidation, Nat. Commun. 15 (2024) 2481.
[38] Q. Sha, S. Wang, L. Yan, Y. Feng, Z. Zhang, S. Li, X. Guo, T. Li, H. Li, Z. Zhuang, D. Zhou, B. Liu, X. Sun, 10,000-h-stable intermittent alkaline seawater electrolysis, Nature 639 (2025) 360–367.
[39] W.J. Weber Jr., J.C. Morris, Kinetics of adsorption on carbon from solution, J. Sanit. Eng. Div. 89 (1963) 31–59.
[40] A.F. Ismail, M.-S. Yim, Investigation of activated carbon adsorbent electrode for electrosorption-based uranium extraction from seawater, Nucl. Eng. Technol. 47 (2015) 579–587.
[41] L. Kong, M. Su, Z. Mai, H. Li, Z. Diao, Y. Xiong, D. Chen, Removal of uranium from aqueous solution by two-dimensional electrosorption reactor, Environ. Technol. Inno. 8 (2017) 57–63.
[42] C.-H. Hou, N.-L. Liu, H.-C. Hsi, Highly porous activated carbons from resource-recovered *Leucaena leucocephala* wood as capacitive deionization electrodes, Chemosphere 141 (2015) 71–79.
[43] C.E. Choong, Y.-Y. Chang, J.-K. Yang, J.R. Kim, S.-E. Oh, Y. Yoon, B.-H. Jeon, E. H. Choi, M. Jang, Fabrication of granular three-dimensional graphene oxide/UiO-66 adsorbent for high uranium adsorption: density functional theory and fixed bed column studies, J. Hazard. Mater. 477 (2024) 135237.
[44] H. Han, J. Hu, X. He, Q. Gao, L. Hu, F. Zhang, K. Zhang, X. Cheng, J. Liu, G. Wu, Development of renewable anti-biofouling UHMWPE fiber-based adsorbents functionalized with amidoxime and polyguanidine salt for uranium extraction from seawater, Sep. Purif. Technol. 364 (2025) 132507.
[45] R. Yu, Y. He, M. An, S. Chen, Y. Ye, L. Li, Superhydrophilic amidoxime-modified poly(vinyl alcohol) fibers for enhanced uranium extraction from seawater, Langmuir 41 (2025) 10516–10525.
[46] X. He, H. Deng, H. Wu, W. Yu, Z. Guo, X. Liang, Amidoxime-based polymer microspheres with high selectivity for uranium from saline Lake brine, ACS Appl. Polym. Mater. 5 (2023) 4380–4387.
[47] C. Namasivayam, K. Ranganathan, Removal of Cd (II) from wastewater by adsorption on "waste" Fe (III) Cr (III) hydroxide, Water Res. 29 (1995) 1737–1744.
[48] P.E. Fanning, M.A. Vannice, A DRIFTS study of the formation of surface groups on carbon by oxidation, Carbon 31 (1993) 721–730.
[49] T. Feng, J. Wu, K. Chai, P. Yang, The anti-biofouling behavior of high voltage pulse electric field (HPEF) mediated by carbon fiber composite coating in seawater, Bioelectrochemistry 123 (2018) 137–144.
[50] X. Guo, H. Yang, Q. Liu, J. Liu, R. Chen, H. Zhang, J. Yu, M. Zhang, R. Li, J. Wang, A chitosan-graphene oxide/ZIF foam with anti-biofouling ability for uranium recovery from seawater, Chem. Eng. J. 382 (2020) 122850.
[51] Z. Liu, H. Zhao, T. Jiang, W. Qin, Influences of marine biofouling on the potential responses of polymeric membrane ion-selective electrodes, Sens. Actuators B 422 (2025) 136692.
[52] Y. Cao, J. Huang, Y. Li, S. Qiu, J. Liu, A. Khasanov, M.A. Khan, D.P. Young, F. Peng, D. Cao, X. Peng, K. Hong, Z. Guo, One-pot melamine derived nitrogen doped magnetic carbon nanoadsorbents with enhanced chromium removal, Carbon 109 (2016) 640–649.
[53] H. Guo, P. Mei, J. Xiao, X. Huang, A. Ishag, Y. Sun, Carbon materials for extraction of uranium from seawater, Chemosphere 278 (2021) 130411.